Science of the Total Environment 739 (2020) 140060

Contents lists available at ScienceDirect

Science of the Total Environment

journal homepage: www.elsevier.com/locate/scitotenv

Evaluation of a high flow rate electrostatic precipitator (ESP) as a particulate matter (PM) collector for toxicity studies

Milad Pirhadi, Amirhosein Mousavi, Constantinos Sioutas *

University of Southern California, Department of Civil and Environmental Engineering, Los Angeles, CA, USA

HIGHLIGHTS

- Application of a high-volume ESP for toxicological studies was investigated.
- Optimum flow and voltage of the ESP was determined in the laboratory.
- ESP can capture semi-volatile species more efficiently than filter sampler.
- Oxidative potential of PM samples collected by ESP was higher than filter.
- Unlike BioSampler, ESP and filter extracts cannot preserve water-insoluble species.

GRAPHICAL ABSTRACT

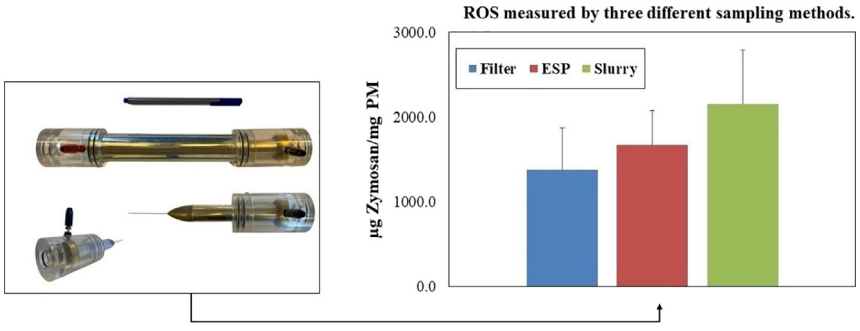

ARTICLE INFO

Article history:
Received 27 March 2020
Received in revised form 20 May 2020
Accepted 5 June 2020
Available online 08 June 2020

Editor: Pavlos Kassomenos

Keywords:
Electrostatic precipitator (ESP)
PM collector
Oxidative potential
Aerosol-into-liquid collection
VACES

ABSTRACT

In this study, we investigated the performance of an electrostatic precipitator (ESP) operating at high flow rates (i.e., 50–100 lpm) as a fine particulate matter ($PM_{2.5}$) collector for toxicological studies. The ESP optimum configuration (i.e., flow rate of 75 lpm and applied voltage of +12 kV) was determined based on maximum particle collection efficiencies and minimum ozone emissions associated with the instrument using different laboratory-generated aerosols. This configuration resulted in particle collection efficiencies above 80% for almost all particles in the size range of 0.015–2.5 μm while the ozone concentration was 17 ppb. The ESP was then deployed to our sampling site in central Los Angeles to evaluate its performance using ambient particles under the optimum configuration. Chemical composition and oxidative potential of $PM_{2.5}$ samples collected on the foils placed inside the ESP tube were compared with those collected concurrently on filters and aerosol slurries using the versatile aerosol concentration enrichment system (VACES) operating in parallel. Our results demonstrated that the ESP was more efficient in preserving labile inorganic ions and total organic carbon (TOC) compared to filters. PM samples collected on ESP substrates also showed higher intrinsic oxidative potential compared to the filters, which might be the result of better preservation of redox active semi-volatile organic compounds on the ESP substrates. However, the TOC concentrations and intrinsic oxidative potential of PM samples collected on ESP substrates were somewhat lower than the aerosol slurries collected by the VACES, probably due to deficiency of water-insoluble compounds in extracted PM samples from ESP substrates. In conclusion, while particle collection for toxicological purposes by the ESP is somewhat inferior to a direct aerosol-into-liquid collection, the ESP performs equally well, if not better, than conventional filter samplers and can be utilized as a simple and adequately efficient PM collector for toxicological studies.

1. Introduction

Particulate matter (PM) has been the focus of several epidemiological and toxicological studies due to its harmful health effects including

* Corresponding author at: 3620 S. Vermont Ave., Los Angeles, CA 90089, USA.
E-mail address: sioutas@usc.edu (C. Sioutas).

https://doi.org/10.1016/j.scitotenv.2020.140060
0048-9697/

respiratory morbidity and mortality, cardiovascular diseases, neurotoxicity, and adverse birth outcomes (Anderson et al., 2012; Anenberg et al., 2010; Nelin et al., 2012; Ostro et al., 2015; Riediker et al., 2004; Sapkota et al., 2010; Wang et al., 2017). In order to investigate the health effects of exposure to ambient PM under controlled conditions, it is necessary to conduct in vitro and in vivo toxicological studies using aerosols representing real-world ambient PM. However, unique and complicated physico-chemical characteristics of real-world PM (e.g., size and chemical composition) cannot be easily replicated by aerosols generated in the laboratory (Keskinen and Rönkkö, 2010; Pirhadi et al., 2018).

The direct use of PM in its typical ambient concentrations is often problematic because these concentrations are not sufficiently high to produce measurable biological impacts in controlled toxicological studies (Lippmann and Chen, 2009). To address this limitation, aerosol concentrators that enrich the concentration of ambient PM by 10–30 fold have been developed and widely used in exposure experiments (Demokritou et al., 2003; Haglund et al., 2002; Kim et al., 2001a, 2001b; Romay et al., 2002). One example is the versatile aerosol concentration enrichment system (VACES) (Kim et al., 2001a, 2001b; Zhao et al., 2005), which employs a saturation-condensation process to grow particles to super-micrometer water droplets, followed by virtual impaction to enrich the concentration of ambient PM at different size ranges by up to 110 fold (Wang et al., 2013a). The concentrated PM can be collected on filters as well as aqueous solutions or be used directly in inhalation chambers, as discussed in several previous studies (Laing et al., 2010; Maciejczyk et al., 2005; Zheng et al., 2015).

Other sampling methods such as high-volume impactors and filter samplers have also been used as alternatives to aerosol concentrators in previous toxicological studies, since they are usually less expensive and easier to handle in comparison to the aerosol concentrators (Demokritou et al., 2002; Kavouras et al., 2000; Misra et al., 2002). Although these high volume instruments are able to collect substantial amounts of ambient PM in short periods of time, they may be associated with sampling artifacts due to the loss of semi-volatile compounds and labile species as well as adsorption of semi-volatile gas phase components during the PM collection (Chow et al., 2010; Kumar and Gupta, 2015; Mader et al., 2001; Nie et al., 2010; Sanderson and Farant, 2005). It should be noted that accurate quantification of ambient semi-volatile components is essential in toxicological studies since these species have major contributions to the overall oxidative potential of ambient PM as demonstrated in earlier studies (Pirhadi et al., 2019a).

More recently, electrostatic precipitators (ESPs), as another approach for PM collection, have been shown to have generally fewer sampling artifacts in comparison to impaction and filtration methods (Han et al., 2009b; Ning et al., 2008; Volckens and Leith, 2002a, 2002b). For example, Volckens and Leith (2002a) reported that by collecting PM samples with ESP, the adsorption of semi-volatile species to its substrate was 5–100 times lower than traditional filter-based particle collection methods. The authors of that study also observed that loss of particles due to evaporation in collecting particles with the ESP was about 2.3 times lower in comparison to particle evaporation from filters. This was attributed to the much smaller surface area of the particulate matter deposit in ESP collectors compared to the effective area of typical fiber filters. Furthermore, ESP collectors offer the advantage of collecting PM samples in long time periods un-attendendly without requiring the regular presence of operators. The majority of previous studies have investigated ESPs with low sampling flow rates (e.g., ≤ 5 lpm) (Mainelis et al., 2002; Ning et al., 2008; Sillanpää et al., 2008; Volckens and Leith, 2002b), which makes them less effective to collect sufficient amounts of PM samples for toxicological studies.

In this study, we have evaluated the performance of a high-flow rate ESP (i.e., with flow rates in the range of 50–100 lpm) as a particle collector for toxicological studies. Cautious steps were taken regarding the ozone emissions associated with the corona discharge of the ESP, as will be further discussed in the manuscript. In order to evaluate the chemical composition and oxidative potential of PM samples collected by the ESP, $PM_{2.5}$ samples were collected in parallel using two other frequently used sampling methods: i) VACES-diffusion dryer collecting PM samples on Teflon filters, and ii) VACES-BioSampler collecting PM samples suspended into aqueous solutions.

2. Methodology

2.1. Design of the ESP

In this study, we utilized a concentric ESP (In-Tox products, LLC, Albuquerque, NM, USA), consisting of an aluminum tube as the collecting electrode and a stainless-steel needle as the discharge electrode located along the column axis. The diameter of the needle was 0.81 mm, and the collecting electrode had a length of 20 cm and a diameter of 3.81 cm. Fig. 1 shows the ESP schematic. The corona needle and two electrodes are also shown in Fig. 1(a). In brief, corona discharge occurs in presence of the considerably strong electric fields so that the free electrons accelerate to such speeds adequate to knock out free electrons from the air molecules and ionize the air accordingly (Malekian et al., 2018). The created ion (coronal) wind then charges the particles on its path effectively. A high voltage power supply (Model Bertran Series 915, Spellman High Voltage Electronics Corp., Hauppauge, NY, USA) was used to apply a positive charge to the discharge electrode, while the collecting electrode was grounded. Fig. S1 shows the current vs voltage experimental curve of the ESP using negative and positive corona voltages. As shown in the figure, for each applied voltage, the measured current for negative voltage is higher than that of positive voltage, which is attributed to the higher ion production and electrical mobility at negative voltages (Niewulis et al., 2013). Higher concentrations of ions in the negative corona configuration would lead to higher particle collection efficiencies as a result of higher number of electrical charges acquired by each particle in this configuration. However, the negative corona produces also higher amounts of ozone (Hinds, 2012) resulting in possible chemical alterations of the collected PM samples (as it will be discussed in Section 2.2). We therefore operated the ESP with a positive corona voltage in order to minimize these artifacts produced by high ozone concentrations.

$PM_{2.5}$ samples were collected on pre-baked aluminum foils (Reynolds Consumer Products LLC, Lake Forest, IL, USA) which were placed carefully on the inner surface of the collecting electrode. The ozone emission levels associated with the ESP corona discharge and the selection of the optimum operational parameters of the ESP such as flow rate and applied voltage (i.e., 75 lpm and 12 kV) will be discussed in detail in the following sections.

2.2. Laboratory experiments

Laboratory experiments were conducted to evaluate and select the optimum operational configuration of the ESP in terms of flow rate and applied voltage based on the range of particle collection efficiencies and associated ozone generation. Fig. 1(b) shows the schematic setup of the laboratory tests. Laboratory-generated polydisperse sodium chloride (NaCl) aerosols with a concentration of 300 μg/ml were prepared by dissolving 15 mg of NaCl powder (3628–01, J. T. Baker, U.S.P. - F.C.C. grade) in 50 ml of ultrapure (Milli-Q) water. The solution was then homogenized by sonicating in an ultrasonic bath (3510R-MT, Branson Ultrasonics Corp., Danbury, CT, USA) for 30 min. Using a HOPE jet nebulizer (Model 11,310, B&B Medical Technologies, Carlsbad, CA, USA) connected to HEPA-filtered compressed air, the solution was atomized into the small droplets. This aerosolized stream was mixed with clean air filtered by a HEPA capsule (Model No. 12144, Pall Laboratory, Port Washington, NY, USA), and passed through a diffusion dryer (Model 3620, TSI Inc., USA) containing pre-baked silica gel in order to remove the excess water vapor from the aerosol and decrease the relative humidity (RH) to around 50%. The electrical charge of the aerosol was also removed by passing through a cylinder supplied with ten Po-

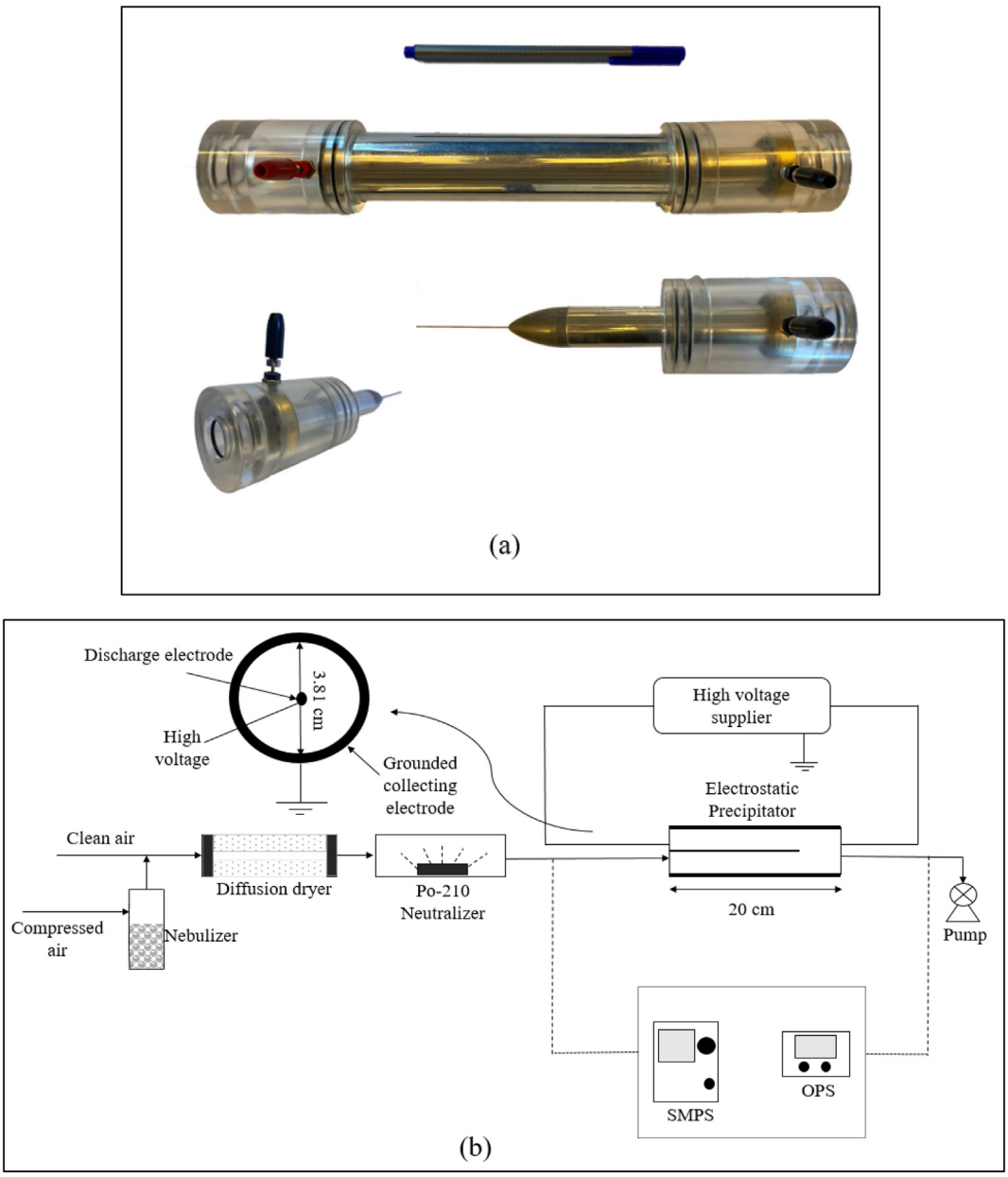

Fig. 1. Electrostatic Precipitator (ESP): a) pictures of the ESP; b) schematic of the laboratory tests for the ESP operation.

210 neutralizers prior to entering the ESP. To calculate the ESP collection efficiency for smaller size ranges (i.e., 0.01 to 0.3 μm), the number-based size distribution of the particles was obtained before and after the ESP by means of a scanning mobility particle sizer (SMPS, Model 3936, TSI Inc., Shoreview, MN, USA) operating in conjunction with a condensation particle counter (CPC, Model 3022A, TSI Inc., Shoreview, MN, USA). Similarly, the collection efficiency for larger size ranges (i.e., 0.3–2.5 μm) was calculated utilizing an optical particle sizer (OPS, Model 3330, TSI Inc., Shoreview, MN, USA).

Prior to performing the ESP collection efficiency tests, the ozone emissions associated with the ESP corona discharge at different flow rates and applied voltages were measured in order to identify an optimum configuration resulting in high collection efficiencies (i.e., over 80–85%) with low ozone generation. Ozone concentrations in the ESP air flow were measured by connecting a UV Photometric O_3 Analyzer (Thermo Environmental Instrument, Model 49C, Franklin, MA, USA) to the exiting air stream from the ESP. Initial calibration was performed using the air stream filtered by a HEPA-filter connected to the instrument. Subsequently, the ozone concentrations in air stream were measured under different operational configurations (i.e., flow rates and applied voltages) of the ESP. Excessive ozone production by the ESP corona discharge in certain configurations might alter the chemical composition of PM samples significantly based on the previous studies (Huang and Chen, 2003; Kaupp and Umlauf, 1992; Volckens and Leith, 2002b). The impact of different flow rates (i.e., 50, 75, and 100 lpm) on the collection efficiency of our ESP design was investigated under the maximum applied voltage (i.e., 12 kV). Subsequently, at the optimum flow rate, the effect of different voltages (i.e., 8, 10, and 12 kV) on the collection efficiency of ESP was evaluated. Lastly, at the optimum configuration of the ESP in terms of maximum collection efficiency with lower ozone generation, additional tests were conducted utilizing monodisperse polystyrene latex (PSL) particles (Polysciences Inc., Warrington, PA, USA) at various size ranges (i.e., 0.3, 0.5, 0.75, 1, and 2 μm) as well as other polydisperse aerosols (i.e., glutaric acid and ammonium nitrate) to confirm that the performance of the ESP is not affected by the chemical composition of the passing aerosols.

2.3. Field experiments

Following optimization of the ESP operational configuration in the laboratory, the ESP was deployed at the particle instrumentation unit (PIU) of University of Southern California for field tests. The PIU is located in central Los Angeles at a distance of ~150 m from the I-110 freeway. Earlier studies have demonstrated that this location represents a typical urban area exposed to ambient PM originating from mostly traffic sources (Soleimanian et al., 2019). Fig. 2(a) and (b) show the schematic of the field test setup for the ESP, and VACES operations, respectively. Concurrent $PM_{2.5}$ samples were collected using the ESP and the two other sampling methods including the VACES-diffusion dryer-filter and VACES-BioSampler for comparison purposes to evaluate the chemical composition and oxidative potential of the $PM_{2.5}$ samples collected by these three different sampling approaches, as mentioned earlier in the Introduction section.

As shown in Fig. 2(a), a 90-degree elbow made of an aluminum tube with a diameter of 0.5 cm was employed as an approximate $PM_{2.5}$ impactor/inlet before the ESP to remove coarse PM (i.e., larger than 2.5 μm) from the air sample. The design and important characteristics of this $PM_{2.5}$ inlet are described in the Supplementary Information (SI) in Section S1.

Details regarding the VACES operation and performance have been elaborated in earlier studies (Kim et al., 2001a, 2001b; Pirhadi et al., 2019b; Zhao et al., 2005). In brief, the ambient particles were drawn with a flow rate of 210 lpm into a pre-impactor with a cut-point of 2.5 μm, and subsequently mixed with water vapor as they passed through a saturation tank at 30 °C. The flow was then split into two lines, each at a flow rate of 105 lpm. In each line, the flow underwent a supersaturation process after passing through a condensation section in which the temperature was decreased to around 21–22 °C, resulting in the condensation of the excess water vapor on the particles and growing the particles to around 3–4 μm. The grown particles in each line then entered a virtual impactor with a cut-point of 1.5 μm and a minor flow rate of 5 lpm, leading to particle concentration enrichment by an approximate factor of 20. In the first line, concentrated particles were drawn into a diffusion dryer (Model 3620, TSI Inc., Shoreview, MN, USA) in order to remove the extra moisture and revert the original size of the particles. These particles were then collected on a 37-mm PTFE (Teflon) filter (Pall Corp., Life Sciences, 2-μm pore, Ann Arbor, MI, USA). In the second line, the grown particles were directly drawn into the BioSampler after the virtual impactor, which collects slurry PM samples by means of impaction and centrifugal forces by injecting the concentrated liquid droplets into a swirling water volume (Daher et al., 2011; Kim et al., 2001a, 2001b). Five sets of PM samples were collected during October–November 2019, and each set of samples included PM slurries from VACES-BioSampler, filters from VACES-diffusion dryer, and foil substrates from the ESP. Each sampling cycle covered approximately 1 week, collecting PM samples for about 7 h a day.

2.4. Gravimetric and chemical analysis

During the field experiments, five sets of PM samples on aluminum foils were collected using the ESP. In parallel with these samples, five sets of PM suspensions, each containing 70 ml, as well as five sets of Teflon filters were collected by the VACES/BioSampler. The mass concentration of PM samples collected by the ESP and filters was calculated by dividing the collected mass on the foils and filters using pre-and post-weighting to the volume of sampled air. The filters and foils were kept for 24 h at a controlled environment with a temperature of 22–24 °C and a relative humidity of 40–50% to ensure their equilibration after each test. Then, the mass of filters was measured by a microbalance (MT5, Mettler-Toledo Inc., USA) with a ± 0.001 mg precision, and the mass of aluminum foils was measured employing a filter balance (LA 130 S-F, Sartorius, Bohemia, NY, USA). The collected PM mass on filters was used as our reference for mass-based normalization of the measured chemical components and oxidative potential in the slurry. As observed in Fig. S4, the mass concentrations of ambient $PM_{2.5}$ samples collected by the VACES-filter sampler based on the gravimetrical measurements were in very good agreement with the reference ambient $PM_{2.5}$ data recorded by the regulatory monitoring stations near our sampling site.

All of the collected $PM_{2.5}$ samples were chemically analyzed for different components including inorganic ions, total organic carbon (TOC), and metals and trace elements by the Wisconsin State Lab of Hygiene (WSLH). To extract PM from the ESP aluminum foils, sonication with high-purity Milli-Q solution (with ~1:10 mixture of methanol and water) was conducted. Since it was not possible to digest the foil and PM directly in the acid mixture, the extraction volume was minimized for enhanced sensitivity. The TOC content of the samples was quantified by means of a Sievers 900 total organic carbon analyzer (Stone et al., 2008). Moreover, inductively coupled plasma mass spectroscopy (ICP-MS) and ion chromatography (IC) were utilized, respectively, in order

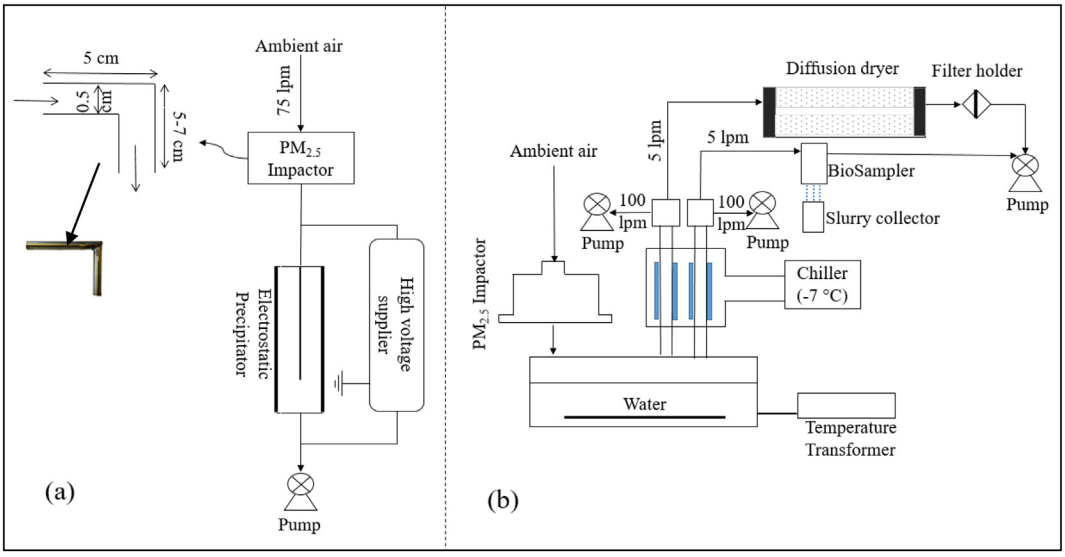

Fig. 2. Schematic of the field tests: a) ESP operation and design parameters as well as the impactor design and picture; b) VACES operation collecting PM samples on a filter and the BioSampler.

to quantify the metals and trace elements content of the PM samples and their inorganic ions (Herner et al., 2006; Karthikeyan and Balasubramanian, 2006; Lough et al., 2005).

2.5. Toxicological analysis

Several toxicological studies have used the metric of oxidative potential to estimate the association of PM with adverse health effects, by measuring the ability of PM to generate reactive oxygen species (ROS) in the cellular structure, which leads to the production of oxidative stress in cells, and consequently, to adverse health outcomes (Esposito et al., 2014; Paszti-Gere et al., 2012; Tao et al., 2003). A number of chemical and biological assays have been used to measure the oxidative potential of airborne particles, among which the macrophage-based ROS assay has been employed in the present study (Bates et al., 2019; Verma et al., 2015). To measure the oxidative potential of PM samples with the ROS assay, fluorogenic DCFH, a cellular membrane-permeable compound, was applied to rodent alveolar macrophage cells and used as a fluorescent probe. PM samples were extracted from the filters to 1 ml of sterilized Milli-Q water, followed by agitation for 16 h at a dark ambient and sonication for 30 min in the room temperature. The alveolar cell line of the rats (NR8383, American Type Culture Collection) was exposed to the extracted PM samples and DCFH-DA (2,7 dichlorodihydrofluorescein diacetate) with a solution concentration of 15 μM. Inside the cellular structure, DCFH-DA is converted to non-fluorescent 2,7 –dichlorodihydrofluorescein (DCFH), and in the presence of reactive oxygen species it becomes oxidized to the highly fluorescent 2, 7-dichlorofluorescein (DCF). Production of DCF is monitored by a microplate reader, and reported in units of fluorescence per PM mass. Several dilutions were utilized for each PM sample to obtain a robust estimate of the ROS production per PM mass of that sample. Zymosan was employed as a positive control that triggers a strong ROS response recognized by the TLR-2 (Toll-like receptors) of macrophage cells. Accordingly, the intrinsic (per PM mass) oxidative potential based on the ROS assay was reported in units of μg Zymosan/mg (Landreman et al., 2008; Shafer et al., 2016) for each sample.

3. Results and discussion

3.1. Laboratory evaluation

3.1.1. ESP ozone generation

As mentioned in the methodology section, before evaluating the ESP performance at different flow rates and applied voltages, the ozone generation associated with different configurations was assessed. Fig. 3 shows the ozone concentrations produced by the ESP at different flow rates (i.e., 50, 75, and 100 lpm) and voltages (i.e., 8, 10, and 12 kV). As demonstrated in the figure, the concentration of ozone decreases substantially by increasing the sampling flow rate. This is due to the higher dilution of the ozone produced by the ESP corona at higher flow rates. For example, by decreasing the ESP flow rate from 75 lpm to 50 lpm at different voltages (i.e., 6–14 kV), the average ozone concentration increases approximately 13.7 ppb. Moreover, a higher applied voltage increases the ozone production, which is in agreement with the findings of previous studies (Huang and Chen, 2003; Ohkubo et al., 1988; Yehia, 2007). This is due to the higher ionization produced by the higher corona discharge of the ESP, leading to higher ozone generation (Castle et al., 1969; Yehia, 2007). For example, at a flow rate of 75 lpm, we observed a 13-ppb increase in the ozone concentration by increasing the applied voltage from 8 kV to 12 kV.

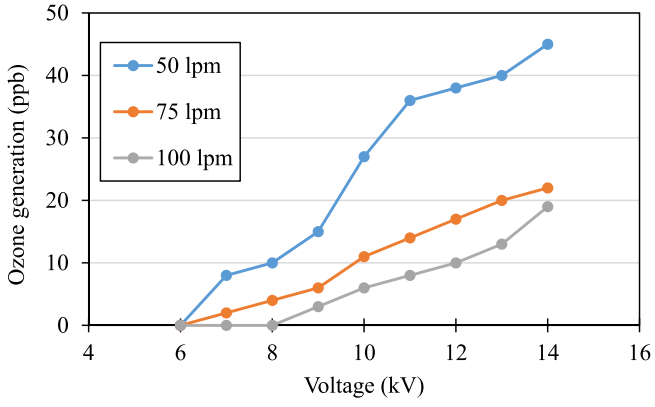

Fig. 3. Ozone concentration in the ESP air stream under different sampling flow rates (i.e., 50, 75, and 100 lpm) and applied positive voltages (i.e., 6–14 kV).

As mentioned earlier, one of the major issues associated with ozone generation in the ESP is the potential artifacts produced by the oxidation of semi-volatile organic compounds under high ozone concentrations that might result in significant changes in the chemical composition of the collected PM (Ning et al., 2008; Volckens and Leith, 2002b). In our ESP, at flow rates in the range of 75–100 lpm, almost all of the ozone concentrations generated by the corona discharge were lower than 20 ppb operating with different applied voltages (i.e., 6–14 kV). The ozone generations observed in this study (i.e., 17 ppb under the optimum configuration of 75 lpm and voltage of 12 kV, which will be discussed in more detail in the next sections of the manuscript) are considerably lower than those of the previous ESP designs (Kaupp and Umlauf, 1992; Ning et al., 2008; Volckens and Leith, 2002b). For example, the observed ozone generations in studies of Kaupp and Umlauf (1992), Volckens and Leith (2002b), and Ning et al. (2008), were around 200–300 ppb, 125 ppb, and 57 ppb, respectively. Volckens & Leith (2002) reported that their ESP, with an associated ozone production of 125 ppb (i.e., around 7 times higher than that of our study), could accurately preserve the chemical composition of important groups of semi-volatile organic components (SVOCs) such as polycyclic aromatic hydrocarbons (PAHs) and alkanes, while there were some errors in characterizing the highly reactive compounds including alkenes. Ning et al. (2008) also reported that the chemical composition of PAHs, hopanes, steranes, and alkanes of the samples collected by their ESP with an ozone production of 57 ppb (i.e., around 3.5 times higher than that of our study), were in very good agreement (i.e., a ratio of 1.07 on average) with those collected by a MOUDI (Micro Orifice Uniform Deposit Impactor) used as a reference sampler. Moreover, the observed ozone production in our ESP (i.e., 17 ppb) is considerably lower than the US EPA (Environmental Protection Agency) air quality standard of 70 ppb for ozone concentrations based on the 8-h averaging time (McCarthy and Shouse, 2018). All of this evidence underpins the notion that the ozone production of 17 ppb under the optimum ESP configuration would likely result in minimal chemical artifacts without causing any adverse health impacts. Results of the chemical composition and oxidative potential for the collected PM samples will be discussed in detail in Section 3.2.

3.1.2. Effect of the ESP sampling flow rate on particle collection efficiency

Fig. 4 illustrates the theoretical and experimental collection efficiencies of the ESP at different flow rates (i.e., 50, 75, and 100 lpm) operating at 12 kV voltage. The equations and related assumptions to calculate the ESP theoretical collection efficiency are explained in detail in the SI in Sections S2 and S3. Based on the figure, our experiments are in good overall agreement with the theoretical calculations of the ESP collection efficiency. The mean absolute errors (MAEs) between the experimental and theoretical collection efficiencies (i.e., the differences between the measured and the calculated values) are equal to 5.8%, 8.8%, and 7.8% for 50, 75, and 100 lpm flow rates, respectively. Part of the difference between the experimental and theoretical collection efficiencies can be explained by the variations of the experimental test data. Another factor is that the theoretical ESP efficiencies were determined for an electrical

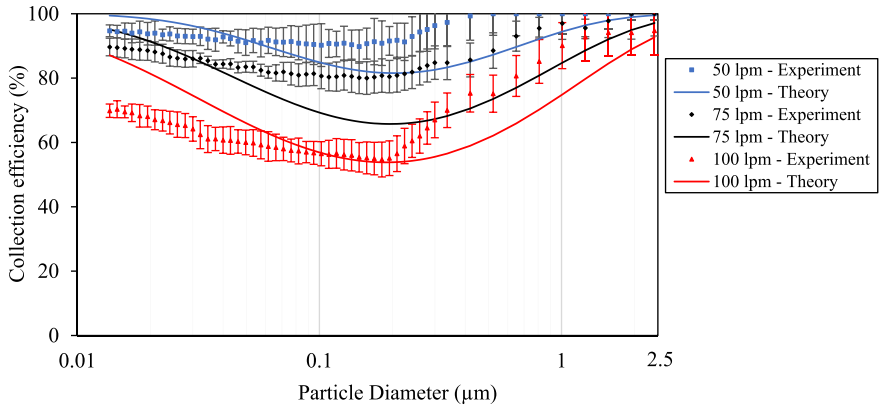

Fig. 4. Experimental particle collection efficiency of the ESP at different size ranges under different flow rates (i.e., 50, 75, and 100 lpm) and at a constant voltage (i.e., +12 kV) using sodium chloride (NaCl) particles, and comparison with theoretical efficiencies. The error bars show one standard error (SE).

field strength value, E, estimated at a single radial distance of 0.75 cm, which is the radius corresponding to the geometric mean of the electrical fields calculated at equally dispersed distances between the inner (i.e., corona centerline) and outer (i.e., collection tube wall) ESP electrodes. We used the geometric mean instead of the arithmetic average because of the exponential decay of the field strength, E, with radial distance (Eq. (5) of the SI). According to the figure, in the smaller size ranges (i.e., d_p < ~80–100 nm), the ESP collection efficiency is higher for smaller particles whereas for larger size ranges (i.e., d_p > 300 nm), the collection efficiency increases with particle diameter. A minimum in the ESP collection efficiency was observed both theoretically as well as experimentally for particles in the range of 100 nm < dp < 200 nm, because this is the range of the lowest particle electrical mobility (Hinds, 2012). This observation is in agreement with the trends reported by previous studies (Huang and Chen, 2003; Ning et al., 2008; Saiyasitpanich et al., 2006; Zhu et al., 2012), which reported minimum collection efficiencies in similar size ranges (~200–350 nm).

The data plotted in Fig. 4 show that at higher flow rates the collection efficiency decreases sharply, as a result of the reduction in the particle residence time in the ESP with increasing flow rates. For example, increasing the flow rate from 75 lpm to 100 lpm resulted in an average 20.1% reduction in the ESP collection efficiency for different size ranges. Similar trends have been observed in earlier studies in the literature (Dramane et al., 2009; Ning et al., 2008; Xu et al., 2015).

Although the particle collection efficiencies observed at the flow rate of 50 lpm were higher than the flow rate of 75 lpm, the associated ozone production at 50 lpm (i.e., 38 ppb) was more than double that at 75 lpm (i.e., 17 ppb) (see Fig. 3). Taking into account the high collection efficiencies at 75 lpm (i.e., around 80–100% for various size ranges) combined with an acceptably low ozone production, we selected 75 lpm as the optimum operational flow rate of our ESP.

3.1.3. Effect of applied voltage

To investigate the effect of applied voltage on the ESP collection efficiency and select the optimum operational voltage, laboratory tests were conducted, as mentioned in Section 2.2. Fig. 5 shows the theoretical and experimental ESP collection efficiencies at different voltages (i.e., 8, 10, and 12 kV) at the optimum flow rate (i.e., 75 lpm). As seen in the figure, the experimentally determined collection efficiencies of the ESP are in good agreement with the theoretical collection efficiencies. MAEs between the experimental collection efficiencies and the theoretical ones for voltages of 8, 10, and 12 kV are 8.4%, 8.6%, and 8.8%, respectively. Moreover, the average standard error (SE) of the experimental collection efficiencies at 8, 10, and 12 kV was 3.5%, 4.1%, and 3.4%, respectively. Similar to the results discussed in Section 3.1.2., the collection efficiency in the smaller size ranges (i.e., d_p < ~80–100 nm) increases with decreasing particle diameter, while in the larger size ranges (i.e., d_p > 300 nm), higher collection efficiencies can be observed with increasing particle diameter. The minimum collection efficiency is once again observed in the size range of 100–200 nm. Furthermore, the collection efficiency of the ESP at different size ranges increases with increasing applied voltage, as expected, since the stronger electrical field at high voltages results in higher particle charging and higher particle electrostatic velocities (Hinds, 2012; Xu et al., 2015). For example, by increasing the voltage from 10 kV to 12 kV, the collection efficiency for different size ranges, on average, increases by about 23%. This is also

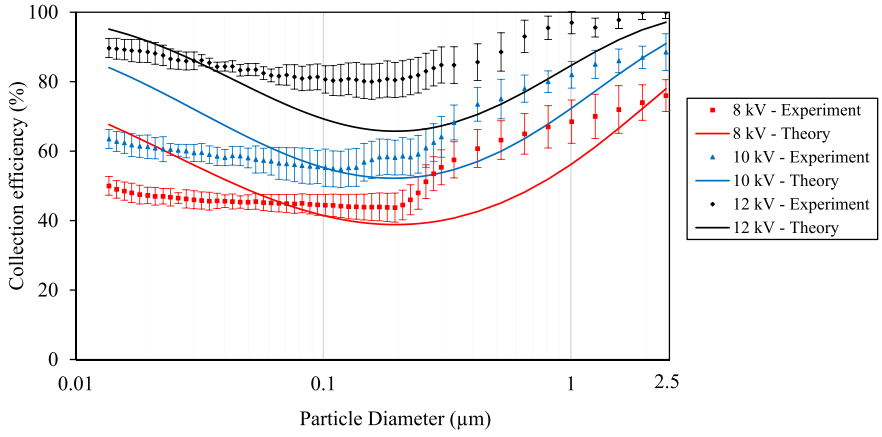

Fig. 5. Experimental particle collection efficiency of the ESP at different size ranges under different voltages of 8, 10, and 12 kV and at a constant flow rate (i.e., 75 lpm) using NaCl aerosols, and comparison with the theoretical collection efficiencies. The error bars show one standard error (SE).

consistent with the results of previous studies using ESP as particle collectors (Niewulis et al., 2013; Zhu et al., 2012).

3.1.4. Effect of particle chemical composition

After determining the optimum operational configuration of the ESP (flow rate of 75 lpm and applied voltage of 12 kV), the ESP performance was further evaluated by aerosolizing particle suspensions of different chemical composition using the same experimental procedure described in Section 2.2. The electrical and hygroscopic properties of aerosols might be altered by changing their chemical composition and mixing state (Bhattu and Tripathi, 2015). The selected laboratory-generated aerosols in this study (e.g., sodium chloride (NaCl), ammonium nitrate (NH_4NO_3), glutaric acid ($C_5H_8O_4$), and polystyrene latex (PSL)) are generally standard particle materials (Blando et al., 2001; Fierz-Schmidhauser et al., 2010; Forsyth et al., 1998; Geller et al., 2005; Gysel et al., 2002; Han et al., 2009a; Matthew et al., 2008). Ammonium nitrate represents one of the most predominant inorganic species that constitute a major fraction of the $PM_{2.5}$ mass in many regions across the world (Lee et al., 2007; Li et al., 2013; Putaud et al., 2004). Moreover, ammonium nitrate is semi-volatile and can be used as a representative of other semi-volatile species in the ambient air (Chang et al., 2000; Verma et al., 2011). Glutaric acid was also selected because it is one of the most common secondary organic compounds created by photo-oxidation of primary emissions in the atmosphere (Kalberer et al., 2000; Stone et al., 2010). Sodium chloride, or sea salt, is a naturally occurring aerosol (Weis and Ewing, 1999). PSL particles are used because of the convenience afforded by their mono-dispersity but also because they represent hydrophobic aerosols compared to the other test aerosols that are largely hygroscopic. Moreover, the selected aerosols cover a wide range of dielectric constants (from about 2.5 for PSL to about 8 for ammonium nitrate (Hinds, 2012; Lee et al., 1996)). Fig. 6 shows the theoretically and experimentally determined values of the ESP collection efficiency for the different types of the test aerosols. According to the data plotted in the figure, the experimental collection efficiencies corresponding to different types of solutions are in good agreement with the theoretical predictions (MAEs are equal to 8.8% 8.1%, 8.8%, and 8.1% for NaCl, ammonium nitrate, glutaric acid, and PSL respectively). The slight differences between the collection efficiencies of different solutions may be attributed to the different electrical permittivity ($\boldsymbol{\varepsilon}$) values between the tested aerosols (Fig. S3). As observed in Fig. 6, the average collection efficiencies for all of the investigated polydisperse and monodisperse aerosols are in the range of about 80–90% for all the size ranges, which corroborated the ESP performance as an efficient PM collector prior to conducting field experiments using ambient PM discussed in the following section.

3.2. Field tests

3.2.1. Chemical composition

Fig. 7 illustrates the mass fraction (i.e., per $PM_{2.5}$ mass concentration) of inorganic ions (i.e., nitrate, sulfate, and ammonium) and TOC for PM samples collected on filters, ESP substrates, and slurries using the VACES-diffusion dryer-filter, ESP, and VACES-BioSampler, respectively. It should be noted that the measured analytical mass of each chemical species was divided by the airborne PM mass of samples collected on ESP substrates and filters prior to the water extraction; this way, any biased representation of enriched concentration of water-soluble species is avoided. As shown in Fig. 7, with the exception of sulfate, the mass contents of TOC and inorganic ions in PM slurry are higher (by 22%, and 28%, respectively) than those collected on the ESP substrate and filter samples, while those of ESP substrate are also higher (by 10%, and 27%, respectively) than filter samples. The TOC concentrations in the PM slurry was 198.6 ± 22.3 μg/mg PM while those of ESP substrate and filter samples were 170.1 ± 22.1 μg/mg PM and 154.9 ± 16.8 μg/mg PM, respectively. The lower mass content of most organic species as well as ammonium nitrate in PM collected on filters compared to those on ESP substrates is probably due to some evaporation of these labile species from the filters, as a result of their higher effective surface area available for particle collection compared to that of the ESP (Ning et al., 2008; Volckens and Leith, 2002b). Additionally, the higher concentration of TOC in PM slurries compared to those collected on ESP substrates and filters can be explained by the more efficient capture of water-insoluble species in the PM slurry (Wang et al., 2013c), compared to the aqueous extraction of PM samples collected on the ESP substrates and filters, which captures mainly the water-soluble compounds. Water-insoluble organic carbon may account for as much as 30–50% of the ambient organic carbon in our sampling site, based on reported values in the previous studies (Pirhadi et al., 2019a; Wang et al., 2013c).

Fig. 8 (a) illustrates a good overall agreement between the mass content of metals and trace elements for PM samples collected on filter, ESP substrate, and slurry. It should be noted that many of these species (e.g., Fe, Mn, Cr, Zn, Ni, V, Cu) are redox-active and thus very important in toxicological studies (Laurent et al., 2016; Shafer et al., 2010). The metal contents of PM extracted from filters and ESP substrates (Fig. 8 (b)), as well as slurries and ESP substrate (Fig. 8 (c)) are highly correlated (i.e., R^2 value of 0.94, and 0.98, respectively) and the slopes of regression lines are close to unity (i.e., slope of 1.16, and 1.26, respectively). It should be noted that PM samples extracted from ESP substrates showed much higher aluminum content compared to those of filters and slurries, which is most probably due to the high aluminum element content in the texture of ESP substrates. Hence, we excluded

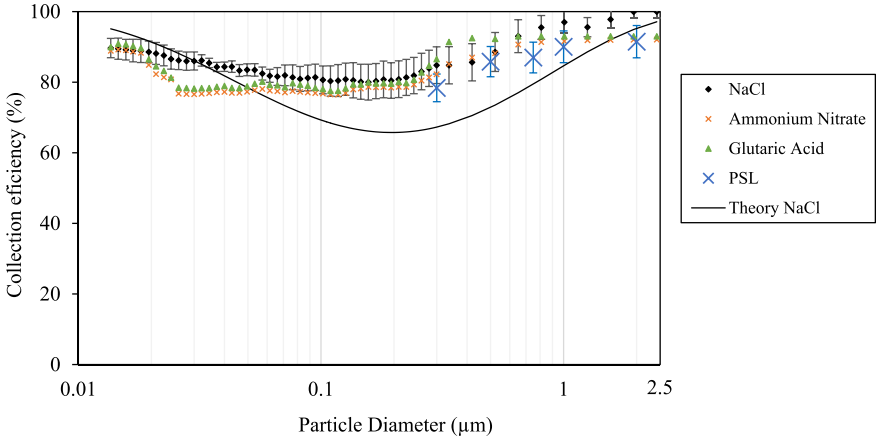

Fig. 6. Experimental collection efficiency of the ESP at different size ranges under the optimum configuration (i.e., flow rate of 75 lpm, applied voltage of +12 kV) using different aerosols, including sodium chloride (NaCl), ammonium nitrate (NH_4NO_3), glutaric acid, and polystyrene latex (PSL), and comparison with the theoretical collection efficiency calculated for NaCl. The standard error (SE) of the data has been shown only for NaCl and PSL solutions, because the experimental uncertainties for the rest of test aerosols were similar.

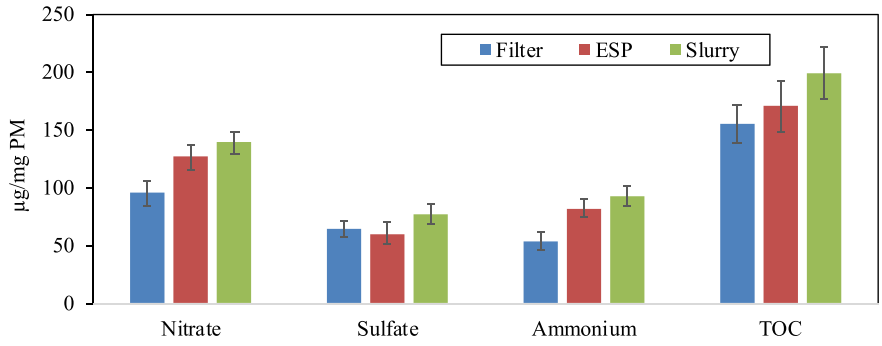

Fig. 7. Average per PM mass fractions of inorganic ions (nitrate, sulfate, and ammonium) and total organic carbon (TOC) for PM samples collected on filters, ESP substrates (after water-extraction), and aqueous slurries. Error bars represent one standard error (SE).

this metal from our correlation analysis. Differences between the concentration of these trace species collected on filters and ESP substrates is within the variation of data, and there is no clear increasing or decreasing trend in the mass content from filter to ESP substrate. Similar to TOC, the higher mass content of metals and trace elements in PM slurries compared to those of substrate samples is again a result of water-insoluble elements inherently collected in the PM slurries, which are inefficiently removed during the water-extraction process from filter and ESP substrate samples.

3.2.2. Oxidative potential of $PM2_{.5}$ collected by the three different sampling methods

Fig. 9 shows the intrinsic oxidative potential (in units of µg Zymosan/mg PM) of the collected PM samples on filters, ESP substrates, and

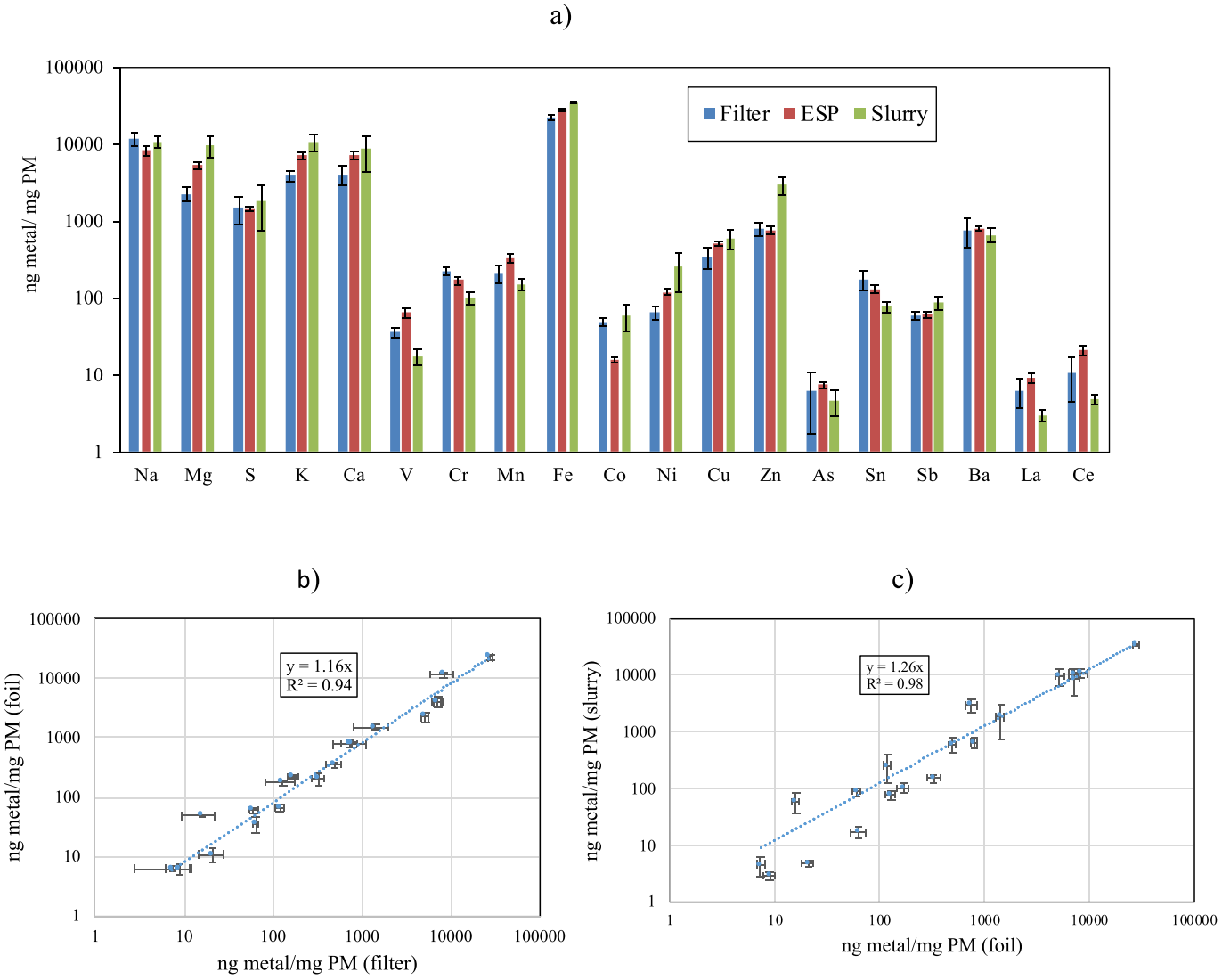

Fig. 8. a) Mass fractions of metals and trace elements of PM samples collected on filters, ESP substrates (water-extracted), and aqueous slurries. b) Correlation between mass fraction of metals and trace elements of PM collected on ESP substrate vs filter, and c) slurry vs ESP substrate for average mass content of different metals. Error bars represent one standard error (SE).

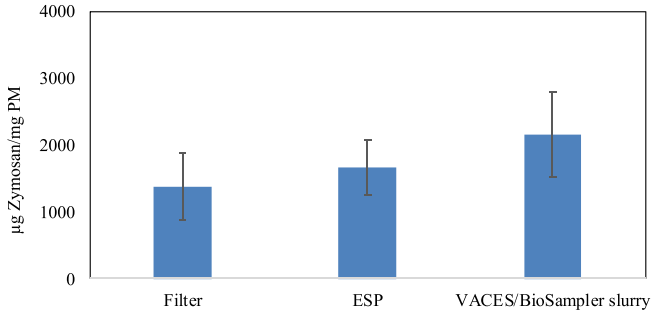

Fig. 9. Average intrinsic (per PM mass) oxidative potential for PM samples collected on filters, ESP substrates (water-extracted), and aqueous slurries. Error bars represent one standard error (SE).

slurries. The oxidative potential of PM samples collected on slurries (2153.9 ± 633.1 μg Zymosan/mg PM) is approximately 30% higher than ESP substrates (1670 ± 410.9 μg Zymosan/mg PM); this is most probably due to the higher content of TOC, especially of water-insoluble organic compounds, in PM slurries, which can be regarded as a notable advantage of this sampling methodology for collecting PM for use in toxicity studies (Wang et al., 2013c, 2013b). Previous studies have documented the redox-activity of organic species (both water soluble and water insoluble) in urban environments (Bae et al., 2017; Bates et al., 2019; Biswas et al., 2009; Delgado-Saborit et al., 2011; Knecht et al., 2013; Pirhadi et al., 2019a; Verma et al., 2009), and the importance of water-insoluble compounds contributing to a considerable fraction of the oxidative potential of $PM_{2.5}$ (Daher et al., 2011; Wang et al., 2013c). Furthermore, the oxidative potential of PM samples collected on the ESP substrates is around 20% higher than that of filters (1374.1 ± 500 μg Zymosan/mg PM), which could be attributed to better preservation of semi-volatile organic components (SVOCs) compared to traditional filters, as argued in earlier investigations (Cardello et al., 2002; Volckens and Leith, 2002a).

Regarding the impact of organic components oxidation on the ROS results, as mentioned earlier, previous ESP studies with significantly higher ozone productions (i.e., 57–125 ppb) compared to our study (i.e., 17 ppb) have reported that the ESP could accurately preserve chemical composition of most of the SVOCs such as PAHs, alkanes, hopanes, and steranes (Ning et al., 2008; Volckens and Leith, 2002b). Furthermore, we did not observe any visible signs of corrosion resulting from the oxidation on the aluminum foils of the ESP substrates (as demonstrated by Volckens and Leith (2002a)) during our sampling campaign. More importantly, if the degree of organics oxidation and the subsequent formation of redox-active secondary organic aerosols (SOAs) was significant (Khan et al., 2016; Tuet et al., 2017), one would expect to observe higher levels of ROS for ESP substrates. However, the intrinsic PM oxidative potential of the samples collected on ESP substrates is still lower than that collected in the aqueous slurries as shown in Fig. 9. Although chemical artifacts associated with the ozone generation of the ESP cannot be ruled out, similar artifacts would likely occur on the PM samples collected on filters because: 1) the airstream entering the filter is not depleted of ozone (since O_3 is not removed from the air sample, and it is therefore at ambient levels as the air sample penetrates the filter), and 2) the air comes into contact with a much larger effective surface area than the ESP substrate. According to the data extracted from the Chemical Speciation Network (CSN) for our sampling location, the average ambient ozone concentration was about 20 ppb during our field campaign (October and November of 2019) (Air Quality Data (PST) Query Tool, 2019), therefore in a range comparable to that produced by the ESP.

4. Summary and conclusions

The objective of this study was to evaluate the performance of an electrostatic precipitator (ESP) operating at high flow rate as a $PM_{2.5}$ collection method for use in toxicological studies. According to the particle collection efficiency and ozone generation measured at the laboratory, the optimum operational flow rate and applied voltage of ESP was determined to be 75 lpm and +12 kV, respectively, resulting in average collection efficiency of ~85% (i.e., $PM_{2.5}$) and ozone concentration of 17 ppb. The aerosol-into-liquid collection of ambient PM by means of the VACES/BioSampler was the most effective method in capturing both redox-active water soluble and insoluble species, resulting in the highest ROS levels among the three sampling methods investigated in this study. Although somewhat inferior to the VACES/BioSampler, the ESP captured labile organic and inorganic species more efficiently than the filter sampler, resulting in higher oxidative potential values compared to filters. Despite the superiority of the VACES/BioSampler system in capturing redox-active PM species, the operational simplicity of the ESP and its higher collection efficiency of labile PM species compared to conventional filtration might make it an attractive alternative for PM collection for toxicological studies.

CRediT authorship contribution statement

Milad Pirhadi: Conceptualization, Methodology, Formal analysis, Data curation, Writing - original draft. **Amirhosein Mousavi:** Investigation, Methodology, Data curation, Validation. **Constantinos Sioutas:** Conceptualization, Project administration, Funding acquisition, Supervision, Resources, Writing - review & editing.

Declaration of competing interest

As the first author of the paper, on behalf of all of the co-authors declares that there are no known competing financial interests or personal relationships that could have appeared to influence the work reported in this paper.

Acknowledgments

This study was supported by the National Institutes of Health (NIH) (grants numbers: 1RF1AG051521-01, 1R01ES024936-01, 1P01AG055367-01A1). We would also like to acknowledge the support of the PhD fellowship award from the USC Viterbi School of Engineering.

Appendix A. Supplementary data

Supplementary data to this article can be found online at https://doi.org/10.1016/j.scitotenv.2020.140060.

References

Air Quality Data (PST) Query Tool, 2019. . WWW Document. URL. https://www.arb.ca.gov/aqmis2/aqdselect.php?tab=specialrpt.

Anderson, J.O., Thundiyil, J.G., Stolbach, A., 2012. Clearing the air: a review of the effects of particulate matter air pollution on human health. J. Med. Toxicol. 8, 166–175. https://doi.org/10.1007/s13181-011-0203-1.

Anenberg, S.C., Horowitz, L.W., Tong, D.Q., West, J.J., 2010. An estimate of the global burden of anthropogenic ozone and fine particulate matter on premature human mortality using atmospheric modeling. Environ. Health Perspect. 118, 1189–1195. https://doi.org/10.1289/ehp.0901220.

Bae, M.-S., Schauer, J.J., Lee, T., Jeong, J.-H., Kim, Y.-K., Ro, C.-U., Song, S.-K., Shon, Z.-H., 2017. Relationship between reactive oxygen species and water-soluble organic compounds: time-resolved benzene carboxylic acids measurement in the coastal area during the KORUS-AQ campaign. Environ. Pollut. 231, 1–12.

Bates, J.T., Fang, T., Verma, V., Zeng, L., Weber, R.J., Tolbert, P.E., ... Russell, A.G., 2019. Review of acellular assays of ambient particulate matter oxidative potential: Methods and relationships with composition, sources, and health effects. Environ. Sci. Technol. 53 (8), 4003–4019.

Bhattu, D., Tripathi, S.N., 2015. CCN closure study: effects of aerosol chemical composition and mixing state. J. Geophys. Res. Atmos. 120, 766–783.

Biswas, S., Verma, V., Schauer, J.J., Cassee, F.R., Cho, A.K., Sioutas, C., 2009. Oxidative potential of semi-volatile and non-volatile particulate matter (PM) from heavy-duty vehicles retrofitted with emission control technologies. Environ. Sci. Technol. 43, 3905–3912.

Blando, J.D., Porcja, R.J., Turpin, B.J., 2001. Issues in the quantitation of functional groups by FTIR spectroscopic analysis of impactor-collected aerosol samples. Aerosol Sci. Technol. 35, 899–908.

Cardello, N., Volckens, J., Tolocka, M.P., Wiener, R., Buckley, T.J., 2002. Performance of a Personal Electrostatic Precipitator Particle Sampler.

Castle, G.S.P., Inculet, I.I., Burgess, K.I., 1969. Ozone generation in positive corona electrostatic precipitators. IEEE Trans. Ind. Gen. Appl. 489–496.

Chang, M.C., Sioutas, C., Kim, S., Gong Jr., H., Linn, W.S., 2000. Reduction of nitrate losses from filter and impactor samplers by means of concentration enrichment. Atmos. Environ. 34, 85–98.

Chow, J.C., Watson, J.G., Chen, L.-W., Rice, J., Frank, N.H., 2010. Quantification of PM 2.5 organic carbon sampling artifacts in US networks. Atmos. Chem. Phys. 10, 5223–5239.

Daher, N., Ning, Z., Cho, A.K., Shafer, M., Schauer, J.J., Sioutas, C., 2011. Comparison of the chemical and oxidative characteristics of particulate matter (PM) collected by different methods: filters, impactors, and BioSamplers. Aerosol Sci. Technol. 45, 1294–1304. https://doi.org/10.1080/02786826.2011.590554.

Delgado-Saborit, J.M., Stark, C., Harrison, R.M., 2011. Carcinogenic potential, levels and sources of polycyclic aromatic hydrocarbon mixtures in indoor and outdoor environments and their implications for air quality standards. Environ. Int. 37, 383–392.

Demokritou, P., Kavouras, I.G., Ferguson, S.T., Koutrakis, P., 2002. Development of a high volume cascade impactor for toxicological and chemical characterization studies. Aerosol Sci. Technol. 36, 925–933.

Demokritou, P., Gupta, T., Ferguson, S., Koutrakis, P., 2003. Development of a high-volume concentrated ambient particles system (CAPS) for human and animal inhalation toxicological studies. Inhal. Toxicol. 15, 111–129.

Dramane, B., Zouzou, N., Moreau, E., Touchard, G., 2009. Electrostatic precipitation in wire-to-cylinder configuration: effect of the high-voltage power supply waveform. J. Electrost. 67, 117–122.

Esposito, S., Tenconi, R., Lelii, M., Preti, V., Nazzari, E., Consolo, S., Patria, M.F., 2014. Possible molecular mechanisms linking air pollution and asthma in children. BMC Pulm. Med. 14, 1–8. https://doi.org/10.1186/1471-2466-14-31.

Fierz-Schmidhauser, R., Zieger, P., Wehrle, G., Jefferson, A., Ogren, J.A., Baltensperger, U., Weingartner, E., 2010. Measurement of relative humidity dependent light scattering of aerosols. Atmos. Meas. Tech. 3, 39–50.

Forsyth, B., Liu, B.Y.H., Romay, F.J., 1998. Particle charge distribution measurement for commonly generated laboratory aerosols. Aerosol Sci. Technol. 28, 489–501.

Geller, M.D., Biswas, S., Fine, P.M., Sioutas, C., 2005. A new compact aerosol concentrator for use in conjunction with low flow-rate continuous aerosol instrumentation. J. Aerosol Sci. 36, 1006–1022.

Gysel, M., Weingartner, E., Baltensperger, U., 2002. Hygroscopicity of aerosol particles at low temperatures. 2. Theoretical and experimental hygroscopic properties of laboratory generated aerosols. Environ. Sci. Technol. 36, 63–68.

Haglund, J.S., Chandra, S., Mcfarland, A.R., 2002. Evaluation of a high volume aerosol concentrator. Sci. Technol. 36, 690–696. https://doi.org/10.1080/0278682029003837.

Han, B., Hudda, N., Ning, Z., Kim, H.-J., Kim, Y.-J., Sioutas, C., 2009a. A novel bipolar charger for submicron aerosol particles using carbon fiber ionizers. J. Aerosol Sci. 40, 285–294.

Han, B., Hudda, N., Ning, Z., Kim, Y.-J., Sioutas, C., 2009b. Efficient collection of atmospheric aerosols with a particle concentrator—electrostatic precipitator sampler. Aerosol Sci. Technol. 43, 757–766.

Herner, J.D., Green, P.G., Kleeman, M.J., 2006. Measuring the trace elemental composition of size-resolved airborne particles. Environ. Sci. Technol. 40, 1925–1933.

Hinds, W.C., 2012. Aerosol Technology: Properties, Behavior, and Measurement of Airborne Particles. John Wiley & Sons.

Huang, S.-H., Chen, C.-C., 2003. Loading characteristics of a miniature wire-plate electrostatic precipitator. Aerosol Sci. Technol. 37, 109–121.

Kalberer, M., Yu, J., Cocker, D.R., Flagan, R.C., Seinfeld, J.H., 2000. Aerosol formation in the cyclohexene-ozone system. Environ. Sci. Technol. 34, 4894–4901. https://doi.org/10.1021/es001180f.

Karthikeyan, S., Balasubramanian, R., 2006. Determination of water-soluble inorganic and organic species in atmospheric fine particulate matter. Microchem. J. 82, 49–55.

Kaupp, H., Umlauf, G., 1992. Atmospheric gas-particle partitioning of organic compounds: comparison of sampling methods. Atmos. Environ. Part A, Gen. Top. 26, 2259–2267. https://doi.org/10.1016/0960-1686(92)90357-Q.

Kavouras, I.G., Ferguson, S.T., Wolfson, J.M., Koutrakis, P., 2000. Development and validation of a high-volume, low-cutoff inertial impactor. Inhal. Toxicol. 12, 35–50.

Keskinen, J., Rönkkö, T., 2010. Can real-world diesel exhaust particle size distribution be reproduced in the laboratory? A critical review. J. Air Waste Manag. Assoc. 60, 1245–1255. https://doi.org/10.3155/1047-3289.60.10.1245.

Khan, M.B., Masiol, M., Formenton, G., Di Gilio, A., de Gennaro, G., Agostinelli, C., Pavoni, B., 2016. Carbonaceous PM2.5 and secondary organic aerosol across the Veneto region (NE Italy). Sci. Total Environ. 542, 172–181.

Kim, Seongheon, Jaques, P.A., Chang, M., Barone, T., Xiong, C., Friedlander, S.K., Sioutas, C., 2001a. Versatile aerosol concentration enrichment system (VACES) for simultaneous in vivo and in vitro evaluation of toxic effects of ultrafine, fine and coarse ambient particles part II: field evaluation. J. Aerosol Sci. 32, 1299–1314. https://doi.org/10.1016/S0021-8502(01)00058-1.

Kim, S., Jaques, P.A., Chang, M., Froines, J.R., Sioutas, C., Barone, T., 2001b. Versatile aerosol concentration enrichment system (VACES) for simultaneous in vivo and in vitro evaluation of toxic effects of ultrafine, fine and coarse ambient particles part I: development and laboratory characterization. J. Aerosol Sci. 32, 1299–1314. https://doi.org/10.1016/S0021-8502(01)00057-X.

Knecht, A.L., Goodale, B.C., Truong, L., Simonich, M.T., Swanson, A.J., Matzke, M.M., Anderson, K.A., Waters, K.M., Tanguay, R.L., 2013. Comparative developmental toxicity of environmentally relevant oxygenated PAHs. Toxicol. Appl. Pharmacol. 271, 266–275.

Kumar, A., Gupta, T., 2015. Development and laboratory performance evaluation of a variable configuration PM1/PM2.5 impaction-based sampler. Aerosol Air Qual. Res. 15, 768–775. https://doi.org/10.4209/aaqr.2014.11.0307.

Laing, S., Wang, G., Briazova, T., Zhang, C., Wang, A., Zheng, Z., Gow, A., Chen, A.F., Rajagopalan, S., Chen, L.C., Sun, Q., Zhang, K., 2010. Airborne particulate matter selectively activates endoplasmic reticulum stress response in the lung and liver tissues. Am. J. Physiol. - Cell Physiol. 299, 736–749. https://doi.org/10.1152/ajpcell.00529.2009.

Landreman, A.P., Shafer, M.M., Hemming, J.C., Hannigan, M.P., Schauer, J.J., 2008. A macrophage-based method for the assessment of the reactive oxygen species (ROS) activity of atmospheric particulate matter (PM) and application to routine (daily-24 h) aerosol monitoring studies. Aerosol Sci. Technol. 42, 946–957.

Laurent, O., Hu, J., Li, L., Kleeman, M.J., Bartell, S.M., Cockburn, M., Escobedo, L., Wu, J., 2016. A statewide nested case–control study of preterm birth and air pollution by source and composition: California, 2001–2008. Environ. Health Perspect. 124, 1479–1486.

Lee, S.-W., Kim, Y.-W., Kim, Y.-K., 1996. Determination of dielectric constant of dielectric particles using negative dielectrophoresis. Proceedings of Conference on Electrical Insulation and Dielectric Phenomena-CEIDP'96. IEEE, pp. 241–244.

Lee, S., Russell, A.G., Baumann, K., 2007. Source apportionment of fine particulate matter in the southeastern United States. J. Air Waste Manage. Assoc. 57, 1123–1135.

Li, X., Yuesi, Wang, Guo, X., Yingfeng, Wang, 2013. Seasonal variation and source apportionment of organic and inorganic compounds in PM2. 5 and PM10 particulates in Beijing, China. J. Environ. Sci. 25, 741–750.

Lippmann, M., Chen, L.C., 2009. Health effects of concentrated ambient air particulate matter (CAPs) and its components. Crit. Rev. Toxicol. https://doi.org/10.3109/10408440903300080.

Lough, G.C., Schauer, J.J., Park, J.S., Shafer, M.M., Deminter, J.T., Weinstein, J.P., 2005. Emissions of metals associated with motor vehicle roadways. Environ. Sci. Technol. 39, 826–836. https://doi.org/10.1021/es048715f.

Maciejczyk, P., Zhong, M., Li, Q., Xiong, J., Nadziejko, C., Chen, L.C., 2005. Effects of subchronic exposures to concentrated ambient particles (CAPs) in mice: II. The design of a CAPs exposure system for biometric telemetry monitoring. Inhal. Toxicol. 17, 189–197. https://doi.org/10.1080/08958370590912743.

Mader, B.T., Flagan, R.C., Seinfeld, J.H., 2001. Sampling atmospheric carbonaceous aerosols using a particle trap impactor/denuder sampler. Environ. Sci. Technol. 35, 4857–4867.

Mainelis, G., Willeke, K., Adhikari, A., Reponen, T., Grinshpun, S.A., 2002. Design and collection efficiency of a new electrostatic precipitator for bioaerosol collection. Aerosol Sci. Technol. 36, 1073–1085. https://doi.org/10.1080/0278682029009221.

Malekian, D., Sajadi, B., Ahmadi, G., Pirhadi, M., 2018. A numerical study of electric force effects on detachment and deposition of particles due to a falling disk. J. Aerosol Sci. 124, 133–145. https://doi.org/10.1016/j.jaerosci.2018.08.001.

Matthew, B.M., Middlebrook, A.M., Onasch, T.B., 2008. Collection efficiencies in an aerodyne aerosol mass spectrometer as a function of particle phase for laboratory generated aerosols. Aerosol Sci. Technol. 42, 884–898.

McCarthy, J.E., Shouse, K.C., 2018. Implementing EPA's 2015 Ozone Air Quality Standards. CRS Rep. 43092.

Misra, C., Kim, S., Shen, S., Sioutas, C., 2002. A high flow rate, very low pressure drop impactor for inertial separation of ultrafine from accumulation mode particles. J. Aerosol Sci. 33, 735–752. https://doi.org/10.1016/S0021-8502(01)00210-5.

Nelin, T.D., Joseph, A.M., Gorr, M.W., Wold, L.E., 2012. Direct and indirect effects of particulate matter on the cardiovascular system. Toxicol. Lett. 208, 293–299. https://doi.org/10.1016/j.toxlet.2011.11.008.

Nie, W., Wang, T., Gao, X., Pathak, R.K., Wang, X., Gao, R., Zhang, Q., Yang, L., Wang, W., 2010. Comparison among filter-based, impactor-based and continuous techniques for measuring atmospheric fine sulfate and nitrate. Atmos. Environ. 44, 4396–4403.

Niewulis, A., Berendt, A., Podliński, J., Mizeraczyk, J., 2013. Electrohydrodynamic flow patterns and collection efficiency in narrow wire-cylinder type electrostatic precipitator. J. Electrost. 71, 808–814.

Ning, Z., Sillanpää, M., Pakbin, P., Sioutas, C., 2008. Field evaluation of a new particle concentrator-electrostatic precipitator system for measuring chemical and toxicological properties of particulate matter. Part. Fibre Toxicol. 5, 15.

Ohkubo, T., Hamasaki, S., Nomoto, Y., Chang, J.S., Adachi, T., 1988. The effect of corona wire heating on the ozone generations in an air cleaning electrostatic precipitator. Conference Record of the 1988 IEEE Industry Applications Society Annual Meeting. IEEE, pp. 1647–1651.

Ostro, B., Hu, J., Goldberg, D., Reynolds, P., Hertz, A., Bernstein, L., Kleeman, M.J., 2015. Associations of mortality with long-term exposures to fine and ultrafine particles, species and sources: results from the California Teachers Study Cohort. Environ. Health Perspect. 123, 549–556.

Paszti-Gere, E., Csibrik-Nemeth, E., Szeker, K., Csizinszky, R., Jakab, C., Galfi, P., 2012. Acute oxidative stress affects IL-8 and TNF-α expression in IPEC-J2 porcine epithelial cells. Inflammation 35, 994–1004. https://doi.org/10.1007/s10753-011-9403-8.

Pirhadi, M., Sajadi, B., Ahmadi, G., Malekian, D., 2018. Phase change and deposition of inhaled droplets in the human nasal cavity under cyclic inspiratory airflow. J. Aerosol Sci. 118, 64–81. https://doi.org/10.1016/j.jaerosci.2018.01.010.

Pirhadi, M., Mousavi, A., Taghvaee, S., Shafer, M.M., Sioutas, C., 2019a. Semi-volatile components of PM2. 5 in an urban environment: volatility profiles and associated oxidative potential. Atmos. Environ. 117197.

Pirhadi, M., Mousavi, A., Taghvaee, S., Sowlat, M.H., Sioutas, C., 2019b. An aerosol concentrator/diffusion battery tandem to concentrate and separate ambient accumulation mode particles for evaluating their toxicological properties. Atmos. Environ. 213, 81–89. https://doi.org/10.1016/j.atmosenv.2019.05.058.

Putaud, J.-P., Raes, F., Van Dingenen, R., Brüggemann, E., Facchini, M.-C., Decesari, S., Fuzzi, S., Gehrig, R., Hüglin, C., Laj, P., 2004. A European aerosol phenomenology—2:

chemical characteristics of particulate matter at kerbside, urban, rural and background sites in Europe. Atmos. Environ. 38, 2579–2595.

Riediker, M., Cascio, W.E., Griggs, T.R., Herbst, M.C., Bromberg, P.A., Neas, L., Williams, R.W., Devlin, R.B., 2004. Particulate matter exposure in cars is associated with cardiovascular effects in healthy young men. Am. J. Respir. Crit. Care Med. 169, 934–940. https://doi.org/10.1164/rccm.200310-1463oc.

Romay, F.J., Roberts, D.L., Marple, V.A., Liu, B.Y.H., Olson, B.A., 2002. A high-performance aerosol concentrator for biological agent detection. Aerosol Sci. Technol. 36, 217–226. https://doi.org/10.1080/027868202753504074.

Saiyasitpanich, P., Keener, T.C., Lu, M., Khang, S.-J., Evans, D.E., 2006. Collection of ultrafine diesel particulate matter (DPM) in cylindrical single-stage wet electrostatic precipitators. Environ. Sci. Technol. 40, 7890–7895.

Sanderson, E.G., Farant, J.-P., 2005. Atmospheric size distribution of PAHs: evidence of a high-volume sampling artifact. Environ. Sci. Technol. 39, 7631–7637.

Sapkota, A., Chelikowsky, A.P., Nachman, K.E., Cohen, A.J., Ritz, B., 2010. Exposure to particulate matter and adverse birth outcomes: a comprehensive review and meta-analysis. Air Qual. Atmos. Heal. 5, 369–381. https://doi.org/10.1007/s11869-010-0106-3.

Shafer, M.M., Perkins, D.A., Antkiewicz, D.S., Stone, E.A., Quraishi, T.A., Schauer, J.J., 2010. Reactive oxygen species activity and chemical speciation of size-fractionated atmospheric particulate matter from Lahore, Pakistan: an important role for transition metals. J. Environ. Monit. 12, 704–715.

Shafer, M.M., Hemming, J.D.C., Antkiewicz, D.S., Schauer, J.J., 2016. Oxidative potential of size-fractionated atmospheric aerosol in urban and rural sites across Europe. Faraday Discuss. 189, 381–405.

Sillanpää, M., Geller, M.D., Phuleria, H.C., Sioutas, C., 2008. High collection efficiency electrostatic precipitator for in vitro cell exposure to concentrated ambient particulate matter (PM). J. Aerosol Sci. 39, 335–347.

Soleimanian, E., Mousavi, A., Taghvaee, S., Shafer, M.M., Sioutas, C., 2019. Impact of secondary and primary particulate matter (PM) sources on the enhanced light absorption by brown carbon (BrC) particles in central Los Angeles. Sci. Total Environ. 135902.

Stone, E.A., Snyder, D.C., Sheesley, R.J., Sullivan, A.P., Weber, R.J., Schauer, J.J., 2008. Source apportionment of fine organic aerosol in Mexico City during the MILAGRO experiment 2006. Atmos. Chem. Phys. 8, 1249–1259.

Stone, E.A., Hedman, C.J., Zhou, J., Mieritz, M., Schauer, J.J., 2010. Insights into the nature of secondary organic aerosol in Mexico City during the MILAGRO experiment 2006. Atmos. Environ. 44, 312–319.

Tao, F., Gonzalez-Flecha, B., Kobzik, L., 2003. Reactive oxygen species in pulmonary inflammation by ambient particulates. Free Radic. Biol. Med. 35, 327–340. https://doi.org/10.1016/S0891-5849(03)00280-6.

Tuet, W.Y., Chen, Y., Fok, S., Champion, J.A., Ng, N.L., 2017. Inflammatory responses to secondary organic aerosols (SOA) generated from biogenic and anthropogenic precursors. Atmos. Chem. Phys. 17, 11423–11440. https://doi.org/10.5194/acp-17-11423-2017.

Verma, V., Ning, Z., Cho, A.K., Schauer, J.J., Shafer, M.M., Sioutas, C., 2009. Redox activity of urban quasi-ultrafine particles from primary and secondary sources. Atmos. Environ. 43, 6360–6368.

Verma, V., Pakbin, P., Cheung, K.L., Cho, A.K., Schauer, J.J., Shafer, M.M., Kleinman, M.T., Sioutas, C., 2011. Physicochemical and oxidative characteristics of semi-volatile components of quasi-ultrafine particles in an urban atmosphere. Atmos. Environ. 45, 1025–1033. https://doi.org/10.1016/j.atmosenv.2010.10.044.

Verma, V., Fang, T., Xu, L., Peltier, R.E., Russell, A.G., Ng, N.L., Weber, R.J., 2015. Organic aerosols associated with the generation of reactive oxygen species (ROS) by water-soluble PM2. 5. Environ. Sci. Technol. 49, 4646–4656.

Volckens, J., Leith, D., 2002a. Filter and electrostatic samplers for semivolatile aerosols: physical artifacts. Environ. Sci. Technol. 36, 4613–4617.

Volckens, J., Leith, D., 2002b. Electrostatic sampler for semivolatile aerosols: chemical artifacts. Environ. Sci. Technol. 4608–4612.

Wang, D., Kam, W., Cheung, K., Pakbin, P., Sioutas, C., 2013a. Development of a two-stage virtual impactor system for high concentration enrichment of ultrafine, PM2. 5, and coarse particulate matter. Aerosol Sci. Technol. 47, 231–238.

Wang, D., Pakbin, P., Saffari, A., Shafer, M.M., Schauer, J.J., Sioutas, C., 2013b. Development and evaluation of a high-volume aerosol-into-liquid collector for fine and ultrafine particulate matter. Aerosol Sci. Technol. 47, 1226–1238. https://doi.org/10.1080/02786826.2013.830693.

Wang, D., Pakbin, P., Shafer, M.M., Antkiewicz, D., Schauer, J.J., Sioutas, C., 2013c. Macrophage reactive oxygen species activity of water-soluble and water-insoluble fractions of ambient coarse, PM2. 5 and ultrafine particulate matter (PM) in Los Angeles. Atmos. Environ. 77, 301–310.

Wang, Y., Xiong, L., Tang, M., 2017. Toxicity of inhaled particulate matter on the central nervous system: neuroinflammation, neuropsychological effects and neurodegenerative disease. J. Appl. Toxicol. 37, 644–667. https://doi.org/10.1002/jat.3451.

Weis, D.D., Ewing, G.E., 1999. Water content and morphology of sodium chloride aerosol particles. J. Geophys. Res. Atmos. 104, 21275–21285.

Xu, X., Gao, X., Yan, P., Zhu, W., Zheng, C., Wang, Y., Luo, Z., Cen, K., 2015. Particle migration and collection in a high-temperature electrostatic precipitator. Sep. Purif. Technol. 143, 184–191.

Yehia, A., 2007. Calculation of ozone generation by positive dc corona discharge in coaxial wire-cylinder reactors. J. Appl. Phys. 101, 23306.

Zhao, Y., Bein, K.J., Wexler, A.S., Misra, C., Fine, P.M., Sioutas, C., 2005. Field evaluation of the versatile aerosol concentration enrichment system (VACES) particle concentrator coupled to the rapid single-particle mass spectrometer (RSMS-3). J. Geophys. Res. Atmos. 110, 1–11. https://doi.org/10.1029/2004JD004644.

Zheng, Z., Zhang, X., Wang, J., Dandekar, A., Kim, H., Qiu, Y., Xu, X., Cui, Y., Wang, A., Chen, L.C., 2015. Exposure to fine airborne particulate matters induces hepatic fibrosis in murine models. J. Hepatol. 63, 1397–1404.

Zhu, J., Zhao, Q., Yao, Y., Luo, S., Guo, X., Zhang, X., Zeng, Y., Yan, K., 2012. Effects of high-voltage power sources on fine particle collection efficiency with an industrial electrostatic precipitator. J. Electrost. 70, 285–291.